Clim. Past Discuss., 9, 435–465, 2013
www.clim-past-discuss.net/9/435/2013/
doi:10.5194/cpd-9-435-2013

Climate
of the Past
Discussions

Assessing the impact of late Pleistocene megafaunal extinctions on global vegetation and climate

M.-O. Brault[1,*], L. A. Mysak[1], H. D. Matthews[2], and C. T. Simmons[1]

[1]Department of Atmospheric and Oceanic Sciences, McGill University, Montreal, Canada
[2]Department of Geography, Planning and Environment, Concordia University, Montreal, Canada
[*]now at: Department of Geography, McGill University, Montreal, Canada

Received: 6 November 2012 – Accepted: 19 November 2012 – Published: 21 January 2013

Correspondence to: M.-O. Brault (marc-olivier.brault@mail.mcgill.ca)

Published by Copernicus Publications on behalf of the European Geosciences Union.

Abstract

The end of the Pleistocene marked a turning point for the Earth system as climate gradually emerged from millennia of severe glaciation in the Northern Hemisphere. It is widely acknowledged that the deglacial climate change coincided with an unprecedented decline in many species of large terrestrial mammals, including the near-total eradication of the woolly mammoth. Due to an herbivorous diet that presumably involved large-scale tree grazing, the mammoth expansion would have accelerated the expansion of dwarf deciduous trees in Siberia and Beringia, thus contributing to the changing climate of the period. In this study, we use the University of Victoria Earth System Climate Model (UVic ESCM) to simulate the possible effects of megafaunal extinctions on Pleistocene climate change. We have explored various hypothetical scenarios of forest expansion in the Northern Continents, quantifying the regional and global biogeophysical effects in terms of changes in surface albedo and air temperature. In particular, we focus our attention on a Maximum Impact Scenario (MIS) which simulates the greatest possible post-extinction reforestation in the model. More realistic experiments include sensitivity tests based on the timing of extinction, the fraction of trees grazed by mammoths, and the size of mammoth habitats. We also show the results of a simulation with free (non-prescribed) atmospheric CO_2. For the MIS, we obtained a surface albedo increase of 0.006, which resulted in a global warming of 0.175 °C. Less extreme scenarios produced smaller global mean temperature changes, though local warming in some locations exceeded 0.3 °C even in the more realistic extinction scenarios. In the free CO_2 simulation, the biogeophysical-induced warming was amplified by a biogeochemical effect whereby the replacement of high-latitude tundra with shrub forest led to a release of soil carbon to the atmosphere and a small atmospheric CO_2 increase. Overall, our results suggest the potential for a small, though non-trivial, effect of megafaunal extinctions on Pleistocene climate change.

1 Introduction

The last few millennia of the Pleistocene epoch (which lasted until approximately 11.7 ky ago) marked an important transitional period as the Earth's climate emerged from extended periods of severe glaciation in the Northern Hemisphere. This transition involved major changes in the land surface configuration as receding continental ice sheets gave way to the expansion of cold-adapted tundra vegetation and, eventually, the appearance of boreal shrub forest and evergreen needleleaf trees. In turn, the expansion of vegetation would have affected climate by altering the surface albedo (i.e., reflectivity) and enhancing land-atmosphere CO_2 exchange (Kabat et al., 2004). This could have either increased or slowed the rate of high-latitude warming and ice sheet erosion.

Coincidentally, the late Pleistocene also staged one of the most significant terrestrial mass extinctions events of the Cenozoic (past 65 million years). In particular, 97 of 150 genera of megafaunal mammals (defined as animals >44 kg) went extinct globally from about 50 thousand years ago until the end of the Pleistocene (Barnosky et al., 2004). The so-called "megaherbivores" have long been thought to play a central role in the maintenance of grasses over the expansion of trees in the Eurasian taiga due to a presumed herbivorous diet that would have involved large-scale tree grazing, in direct analogy to the actions of present-day megafauna in the African savanna (Owen-Smith, 1987). For example, today a large elephant in South Africa consumes 300 kg of vegetation daily (U. Schutte, personal communication, 2012). Therefore, the extinction of the Pleistocene megafauna could have allowed an additional increase in high-latitude tree cover during the last deglaciation – and therefore a potential change in climate – that would not have occurred otherwise.

The exact cause of the Late Quaternary Extinctions is still subject to an active debate, with a lack of general consensus on the competing hypotheses of natural climate change and a forced change due to human activity (Koch and Barnosky, 2006; Prescott et al., 2012). The occasional presence of woolly mammoth (*Mammuthus primigenius*) remains in paleolithic sites has notably led to the development of various theories attributing the disappearance of the pre-historic mammal to over-hunting by humans (Guthrie, 2006; Alroy, 2001; Martin, 2005). Still, the evidence is not overwhelming and many dismiss the “overkill” hypothesis on the basis that the primitive tools used during the period combined with the woolly mammoth’s thick layer of fat, skin and fur would have made effective hunting by humans unlikely (Grayson and Meltzer, 2002; Wroe et al., 2004).

Assuming humans did have the capacity to overhunt mammoth and significantly reduce their population, Doughty et al. (2010, hereafter DWF2010) hypothesized that the extinction of the woolly mammoth could have led to an expansion of high-latitude forest, and a resulting climate warming due to the corresponding decrease in surface albedo. The assertion that megafaunal extinctions coincided with major regional changes in vegetation is supported by pollen records from a well-documented increase of *Betula* cover in Siberia and Beringia (Global Pollen Database) and data from a collection of Alaskan mammoth fossils (Guthrie, 2006). Based on this evidence, as well as the combined results of a predator-prey model and a global climate model, DWF2010 suggested that a human-driven mammoth extinction could constitute an early case of human-induced climate change and a potential pre-agricultural beginning for the Anthropocene.

Following on from the work of DWF2010, we have simulated the potential impact of megafaunal extinctions on the deglacial climate of the late Pleistocene, extending upon the modeling efforts of DWF2010 in three ways. First, we have examined the transient, long-term climate response to changes in vegetation cover. Second, we have simulated this transient climate change using the multi-component University of Victoria Earth System Climate Model (UVic ESCM), considering boundary conditions relevant to the late Pleistocene (in terms of orbital parameters, ice sheets, and wind fields), as well as transient changes in ocean circulation and heat uptake. Finally, we have included a dynamic treatment of vegetation processes – as opposed to a direct prescription of vegetation cover change – where pre-extinction tree grazing by the woolly mammoths is characterized as a constraint on vegetation growth.

We first analyze results from a maximum impact scenario (henceforth MIS) in which all trees and shrubs are initially assumed to be cleared in a pre-defined mammoth habitat, thus yielding the largest possible climate response in the UVic model resulting from the megafaunal extinctions. Atmospheric CO_2 levels are prescribed in order to eliminate biogeochemical effects, producing a climate response dominated by biogeophysical effects. Following this, we will discuss a range of experiments testing model sensitivity to the timing of extinction, tree grazing fraction, and extent of mammoth habitats. Finally, we compare the biogeophysical and biogeochemical effects of extinction-induced vegetation changes on climate by simulating free carbon cycle interactions within the Earth system.

This paper is structured as follows. In Sect. 2, we give a brief overview of the climatic impact of high latitude vegetation cover change. A short description of the UVic ESCM and the vegetation module are given in Sect. 3. Section 4 discusses the experimental context and the methodology used in this study. In Sect. 5 we shall give an analysis of the MIS, while all other experiments will be briefly overviewed in Sect. 6. Finally, some concluding remarks are given in Sect. 7.

2 A review of climate-vegetation interaction at high latitudes

The climate impact of forests at high latitudes is dominated by radiative effects that arise from vegetation-induced alterations in surface albedo (Foley et al., 2003). This can be partially attributed to the limited amount of moisture in these regions, which reduces the relative importance of heat losses through evapotranspiration. Additionally, there is a very large contrast in surface reflectivity between the dark forest canopy and bare or grass-covered ground, which is amplified by the presence of snow during the colder months. Furthermore, the impact on surface air temperature is enhanced by an important radiative feedback whereby the warming brought about by the expanding tree cover favors an early snow melt during the spring season, resulting in higher temperatures that further promote the spread of vegetation.

The climatic impact of high-latitude vegetation has been analyzed extensively with a variety of numerical models (see, for example, Brovkin et al., 2003; Crucifix et al., 2005). Thomas and Rowntree (1992) were among the first to simulate high-latitude deforestation, associating the wintertime and springtime increased surface albedo (due to reduced tree cover) with a cooling at the surface, negatively impacting not only temperature but also precipitation amounts in the concerned regions, especially around the time of snow melt. Using an explicit scheme prescribing the complete removal of forests at northern high latitudes, Bonan et al. (1992) found that this cooling effect could be extended well beyond the deforested area due to sea ice-albedo feedbacks, and that cool anomalies tended to persist throughout the entire year due to the ocean's thermal inertia. Subsequent studies with the same experimental setup (Bonan et al., 1995; Douville and Royer, 1997) confirmed these findings and hinted at significant climatic impacts of the vegetation change in other parts of the globe, notably in terms of tropical monsoonal circulation. Finally, Snyder et al. (2004) established that boreal forests produced the largest temperature signal of all the major biomes on Earth, including tropical forests.

Climate-vegetation interactions have also been investigated with the much higher resolution regional climate models, allowing for a more diverse representation of subcontinent-scale (e.g., orographic) forcings and thus a better assessment of the impact of localized land surface perturbation. An early example can be found in Chalita and Le Treut (1994), who examined the impact of increased albedo due to deforestation on temperature and precipitation patterns in Europe. Their results suggest a seasonal spread of precipitation inconsistent with global modeling experiments, namely a dry spring followed by a wet summer. These results were further confirmed by another regional climate model study in Europe (Heck et al., 2001). Focusing on the eastern half of Russia, Notaro and Liu (2008) found that local deforestation led to an extended snow cover period and increased atmospheric stability, strengthening the Siberian High and thus decreasing convective precipitation in the region.

There have been a number of global-scale investigations of climate-biosphere interactions in order to evaluate the impact of high-latitude vegetation cover on global climate, and to compare its effect with that of the (more widely studied) tropical forests (Fraedrich et al., 2005; Gibbard et al., 2005; Bala et al., 2007; Brovkin et al., 2009). Results from these experiments suggest that the climatic impacts of the world's vegetation are dominated by radiative effects at mid to high latitudes. More explicitly, Davin and de Noblet-Ducoudré (2010) show that the impact of the change in surface albedo outweighs that of all other biogeophysical effects associated with land cover change.

Finally, it is almost impossible to overlook the importance of vegetation in regulating atmospheric carbon dioxide levels and maintaining the carbon cycle. This is achieved through carbon sequestration and plant photosynthesis, as well as carbon exchanges with the soil layer. The reverse is also true, as vegetation can also be affected by changes in atmospheric carbon dioxide – not only from its direct impact on global surface temperatures, but also due to the central role of the CO_2 molecule in the chemical reactions that define plant life (Prentice et al., 1991). For example, a known impact of elevated atmospheric CO_2 levels is to cause physiological changes such as a reduction of plant stomatal conductance, which limits moisture exchanges between the plant and its environment (Foley et al., 1996). Therefore, the role of vegetation within the carbon cycle is of considerable relevance to any investigation of CO_2 variations and climate change.

3 Model description

The model used in this study is version 2.9 of the University of Victoria Earth System Climate Model (henceforth UVic ESCM, or UVic model), an intermediate complexity coupled atmosphere/ocean/sea-ice model described in great detail in Weaver et al. (2001). The ocean component of the model is version 2.2 of the GFDL Modular

Ocean Model (MOM), a three-dimensional ocean general circulation model with 19 unequally spaced vertical levels. The atmosphere is a vertically-integrated energy-moisture balance model first introduced and coupled to the MOM in Fanning and Weaver (1996), and simplified in Weaver et al. (2001). A specified lapse rate is applied over land to calculate temperature and precipitation anomalies due to orography. Moisture advection is driven by diffusion and by vertically-integrated atmospheric winds specified from NCEP reanalysis data, and a dynamic wind feedback parameterization based on variations in sea surface temperatures is included to account for wind perturbations in past climate simulations. Sea ice is calculated with a standard model involving two-category (sea ice, open water) thermodynamics and elastic-viscous plastic dynamics, with further options available for a more sophisticated representation of sea-ice thermodynamics and ice thickness distributions as described in Bitz et al. (2001). Continental ice consists of a simple prescription of the spatial coverage and height of ice sheets based on data from the model ICE-4G (Peltier, 1994). Finally, the land-sea configuration used in all sub-components operates in a global spatial domain with a spherical grid resolution of 3.6° (zonal) by 1.8° (meridional), which is comparable to most coupled coarse-resolution AOGCM's.

In the current version of the UVic ESCM land surface properties (surface temperature, soil temperature and moisture content, and snow cover) and soil carbon content are computed with a single (1-m) soil layer version of the Meteorological Office Surface Exchange Scheme version 2 (MOSES-2), driven by biomass input and microbial respiration (Cox et al., 1999). Also included in MOSES-2 are an interactive representation of plant photosynthesis and conductance, and a parameterization of evapotranspiration as a function of canopy resistance. Other model expansions found in the newer versions include an improved radiative transfer scheme, the addition of sulfates and aerosols as potential climate forcings (Matthews et al., 2004), the introduction of a dynamic vegetation model (see below), and a coupling of the latter's terrestrial carbon cycle with the ocean's inorganic carbon cycle (Matthews et al., 2005). More recently, modules for ocean biogeochemistry (Schmittner et al., 2008) and ocean sediment deposition and dissolution (Eby et al., 2009) have also been incorporated into the UVic ESCM.

The terrestrial biosphere is represented with the vegetation module "TRIFFID" (Top-down Representation of Interactive Foliage and Flora Including Dynamics), a dynamic global vegetation model developed at the Hadley Centre for use in climate-carbon cycle simulations (Cox, 2001), and adapted to the UVic model by Meissner et al. (2003). It describes the state of the terrestrial biosphere in terms of soil carbon (one-layer) and vegetation distribution, which is expressed through the structure and coverage of five plant functional types (PFT): broadleaf trees, needleleaf trees, C3 and C4 grasses (mainly distinguished by their photosynthesis patterns; C4 is found almost exclusively in the tropics), and shrubs (defined as trees whose maturity height does not exceed 2 m). Plant distribution and soil carbon levels are updated according to a "carbon balance" approach, which is based on primary productivity and land-atmosphere carbon fluxes supplied by the land surface scheme MOSES-2. Areal coverage is determined by the net available carbon and interspecies competition, which is modeled using a Lotka-Volterra predator-prey relationship. In particular, the plant dominance hierarchy heavily emphasizes the role of height in the competition for areal surface, favoring the growth of trees over shrubs and grasses, and shrubs over grasses. The model also accounts for bud-burst, leaf-drop and large-scale vegetation disturbances that increase the soil carbon content.

Finally, most of the model simulations were carried out using a pre-defined time-series of atmospheric CO^2 obtained from Vostok ice cores (Petit et al., 1999) in order to eliminate biogeochemical effects from the change in vegetation cover that might also have an impact on temperature. The initial conditions for these simulations were obtained from the experiments presented in Simmons et al. (2012). These experiments were, in turn, derived from a spin-up for 21 000 BC (23 000 BP) run for 10 000 model years with Last Glacial Maximum (~ 19 000 BC) ice cover (ICE4G), orbital forcing and atmospheric CO^2 fixed for 21 000 BC. This spin-up was then used as the basis for transient simulations from 21 000 BC to 2000 AD. The initial conditions for the present study were then derived from one such transient simulation using time-dependent orbital forcing, prescribed land ice (ICE4G) and prescribed CO_2 (Vostok) at the start dates (15 000 BC–10 000 BC) for the simulations described in this paper.

4 Experimental setup

In this study we examined the climate impacts of the megafaunal extinction, which we represented as an increase in high-latitude tree cover (following the hypothesis formulated in DWF2010). In order to simulate an additional increase in tree cover not caused by existing processes in the model, we devised a "cut-and-grow" setup in which a predefined "mammoth area" would be initially deforested (physically, this approach can be justified by arguing the grazing of trees by terrestrial fauna is not accounted for in the current version of the model), and in these regions trees would only be allowed to grow back following the mammoth extinction. The climatic impacts of forest recovery in the "mammoth area" could then be used to quantify the biogeophysical and/or biogeochemical effects associated with the megafaunal extinction.

In the context of the PFT approach in TRIFFID, the experimental setup limited the growth of trees and shrubs in favor of C3 and C4 grasses over the specified "mammoth area", much in the same way as one would account for agricultural lands in the present-day configuration of vegetation. Once in equilibrium with most other model components (preliminary tests with the UVic ESCM revealed that 500 yr of model simulation were sufficient to reach an approximate steady-state when perturbing an already spun-up model), this constraint to high-latitude tree cover was then removed – either as a sudden or prolonged event, depending on the experiment – in an effort to reproduce the extinction patterns of the woolly mammoth. Due to the strong dominance of tree and shrub PFT in the competition scheme, it took but a few hundred years for boreal forests to recover from their perturbed state. In order to isolate the climate response due to biogeophysical effects only, it was necessary to compare the output of the extinction scenario EXT with that of a "no extinction" simulation CTL, in which the constraint on trees and shrubs was maintained for the duration of the simulation (all other aspects of the simulation remaining unchanged from EXT). Unless otherwise indicated, all figures presented below represent the departure between a simulation EXT and its corresponding CTL run.

5 The Maximum Impact Scenario (MIS)

In this experiment we defined the mammoth area as any land grid cell located north of the 30° N latitude, representing the approximate southernmost limit of boreal forests in the model's Northern Hemisphere. Also, most of the vegetation in North America is constrained between 30° N and 45° N due to the overwhelming presence of the Laurentide ice sheet at higher latitudes during the late Pleistocene. Within the mammoth area, we assumed a complete grazing of non-grass vegetation, which was simulated by setting the effective pre-extinction tree and shrub fraction to zero. Finally, the extinction itself was assumed to occur over a single model time step (i.e., instantaneously), in order to minimize the time required for forest biomes to approximately regain their equilibrium state. The catastrophic event was taken to occur during the year 12 000 BC (14 ky BP), as suggested by the evidence from various burial sites (Guthrie, 2006). In the following sub-sections, we will examine the evolution of surface albedo and air temperature over the following 500 yr (from 14 ky BP to 13.5 ky BP). We emphasize that the MIS does not represent a realistic scenario in terms of actual megafaunal extinction; rather, it models the greatest conceivable influence of megafauna on late Pleistocene climate in the UVic model. Other more realistic experiments will be discussed later.

5.1 Vegetation and surface albedo

The change in the fractions of trees, grasses and shrubs over the mammoth area (Fig. 1a) displays two interesting features. First, we note that the major part of vegetation change occurs within the first 100 yr of the simulation. The expansion of the boreal forest is hastened by the height-based plant dominance hierarchy in the TRIFFID competition scheme, which heavily emphasizes the growth of trees and shrubs over grasses. Second, the forest recovery (which extends to the southern limit of 30° N) is heavily dominated by the shrub PFT, and needleleaf trees only start appearing in Europe and southwestern North America during the last century of the simulation. This result does not contradict the conclusions of DWF2010: based on physical and physiological properties (height, notably), the PFT best representing the *Betula* species would likely be the shrub type in TRIFFID.

The time evolution of surface albedo (Fig. 1b) is found to closely follow the change in vegetation. After 500 yr of climate model simulations, the change in surface albedo due to biogeophysical effects alone amounts to −0.026 locally (mammoth area), and approximately −0.006 globally. The spatial distribution of this increase in albedo is displayed in Fig. 2a. A large area of North America is unavailable for tree growth due to the presence of the vast Laurentide ice sheet (see Fig. 2b). Furthermore, in the model several places in Asia are either too cold (in Northern Siberia) or too dry (all of southern Asia, with the notable exception of the Himalayan mountain range) to support tree growth. This limits extent of shrub forests to a longitudinal band of land stretching from Europe to the Pacific coast and western Alaska, as well as several high-elevation locations (the Himalayas in Asia and Rocky Mountains in North America).

Since shrubs are very similar to grasses in terms of snow-free surface reflectivity, most of the observed albedo decrease is caused by a difference in snow-covered canopy albedo (0.6 for grasses vs. 0.4 for shrubs). This conjecture is validated in the annual spread of surface albedo anomalies in the Northern Hemisphere (Fig. 2c): the departure in surface albedo, largest at the reforested latitudes, all but vanishes during summer and early fall when the ground becomes snow free. In the context of late Pleistocene boundary conditions, the postglacial climate regime in the Northern Hemisphere results in a much later spring snowmelt compared to the present day, as characterized by albedo anomalies that persist until mid-June at these latitudes. The contrast is obvious when considering, for example, the simulations of Thomas and Rowntree (1992), and Chalita and Le Treut (1994), in which present-day boundary conditions result in a March or April snowpack melt. According to Fig. 2c, the (negative) surface albedo anomaly in the reforested latitudes is largest at the end of the spring season. An analysis of seasonal SAT anomalies (see Fig. 3c below) and land surface temperature anomalies (not shown) also reveals that during the same time period this region is much warmer in the reforestation run (EXT) than in the control run (CTL). We interpret these findings as a possible indication that the darker canopy of dwarf trees leads to an earlier spring, and snow melt is hastened by up to a few weeks due to the snow-albedo feedback.

5.2 Temperature

The change in temperature due to biogeophysical effects only is displayed in the form of a globally averaged timeseries of SAT anomalies (Fig. 3a). As expected, the temperature and surface albedo trends are well-correlated, and 500 yr into the simulation the temperature anomaly is approximately 0.175 °C globally and 0.42 °C over the mammoth area. Following the initial, 100-yr increase associated with the northward expansion of shrubs, the temperature (and albedo) anomalies are found to further depart from their pre-extinction values, albeit at a reduced rate. This additional warming fits well into the context of natural deglacial climate change, which causes ice sheets to recede and the land surface to become increasingly hospitable. In the EXT simulation this promotes further expansion of tree and shrub types, in increasing contrast with the CTL simulation in which these PFTs are not allowed to expand north. Because the postglacial warming period extends well into the Holocene, it is likely that the resulting temperature departure between the two simulations would continue increasing well beyond the 500 yr of this simulation.

Not surprisingly, the temperature change obtained at the end of the MIS simulation is several times larger than in the results of DWF2010, who obtained a 0.026 °C warming with a 6 % increase in Siberian tree cover. However, given the fact that our MIS effectively compares 0 % against 100 % tree cover, and that the area of impact is larger in the present study, it is difficult to establish the validity of our results based on a direct comparison with DWF2010. Nevertheless, our results at the very least reinforce the idea that a postglacial expansion of high-latitude vegetation (possibly caused by the extinction of the Pleistocene megafauna) resulted in regional and global warming, contributing to the deglacial climate change of the period.

In general, the spatial patterns of temperature (Fig. 3b) and albedo (Fig. 2a) correspond well, and the maximum temperature anomalies tend to be centered about the reforested areas (negative anomalies in Fig. 2a). The temperature response is not fully linear, however, and two cases stand out: a large temperature departure in eastern Siberia and cooling in the Southern Ocean.

The largest temperature departure (∼ 0.6 °C) can be found in extreme northeast Asia, despite a change in surface albedo comparable to that in central Europe where only half as much warming is observed. We conjecture that the temperature response is enhanced through a particularly long-lasting snow-albedo feedback because of its geographical location, promoting warmer temperatures during most of the year. As mentioned above, there is compelling reason to believe that the warmer spring temperatures due to biogeophysical effects hasten the snowpack melt by a few weeks, creating a very large albedo difference during the late spring and early summer, when temperature is the most sensitive to surface reflectivity.

The above assertion is further supported by the annual spread of temperature anomalies (Fig. 3c). Although the peak anomalies tend to occur later due to the cooler glacial climate, the seasonal cycle is very consistent with results from earlier studies (Thomas and Rowntree, 1992; Bonan et al., 1992; Douville and Royer, 1996), and successfully reproduces the major seasonal variations of temperature.

The second area of interest is situated in the Weddell Sea, off the Antarctic shoreline, where a negative temperature anomaly is observed as a result of warming in the Northern Hemisphere. While it is generally expected that this area should see little change as a result of forcing in the NH, this particular phenomenon is recognized as a direct consequence of a change in oceanic circulation brought about by warm SST anomalies in the North Atlantic. An analysis of the modeled ^{14}C content of the deep waters in the Weddell Sea at the end of the simulation (Fig. 4) reveals a strengthening vertical gradient of δ^{14}C along with a reduced ^{14}C ratio in the bottom waters, often indicative of reduced deep water formation in the Southern Ocean and reduced heat transfer from ocean to atmosphere. These cooler, more stratified surface waters can also lead to increased sea ice formation, triggering a local sea ice-albedo feedback with negative impacts on temperature (and providing a possible explanation to the positive albedo anomalies near the coast of Antarctica as seen in Fig. 2a). The combination of all of the above factors would then explain why this region could experience cooling despite a major warming in the Northern Hemisphere.

6 Results of other experiments

6.1 Intermediate-impact scenarios and sensitivity tests

In this section we present a set of simulations that explore a more realistic range of boundary conditions (compared to the above MIS), taking into account the large uncertainty regarding megafaunal diet, habitat range, and timing of extinction.

The experiments discussed here focus on the impact of three independent aspects: the rate of tree clearing (referred to as “herbivory” in some papers), the spatial extent of mammoth influence on vegetation, and the timing of extinction. The first of these aspects is represented here as a constraint on the growth of tree and shrub PFT, limiting (but not suppressing) their maximum fractional cover over the mammoth area. The second aspect is treated simply as a northward shift of the southernmost limit of the mammoths’ habitat. While perhaps a crude reconstruction, we argue that it is a reasonable approximation given the sparse paleodata available on the spatial distribution of megafaunal populations. The last of these aspects consists of launching the simulation at a different time (with different boundary conditions) in order for the extinction to occur in a different context of natural climate variability; in particular, we desired to test whether any significant change can arise from the experiment being conducted at a different stage of deglacial climate change.

Six individual simulations have been selected for presentation in order to outline the results from this sensitivity study, two from each of the three parameters described above. The details of each experiment are presented in Table 1, which also includes the MIS for the sake of comparison.

In general, model results from the sensitivity tests (Fig. 5) correspond well with our intuition. Decreased herbivory and tree grazing effectively decreased the albedo change (when compared to the "no extinction" run), resulting in less temperature increase. Interestingly, decreasing herbivory by 30 % approximately halved the impact on global temperature, while a 60 % reduction yielded anomalies that were barely distinguishable from the "no-extinction" control simulation. All of the main features of the MIS – the geographical distribution of anomalies, the large departure in eastern Siberia and the Southern Ocean cooling – could be retrieved for these experiments, with proportionately smaller values.

Results from sensitivity to the geographical boundaries of the mammoth area are also fairly straightforward in their interpretation. In reducing the size of mammoth habitat, all potential input from excluded areas (in terms of radiative effects) effectively vanished. Displacing the southern boundary to 45° N reduced the impact by about half, while fixing it at 60° N all but negated biogeophysical effects as there are very few ice-free locations north of this boundary that can support the expansion of vegetation. In every case the model output displayed broad similarities with the MIS, reproducing the notable temperature anomalies both in eastern Siberia and in the Southern Ocean.

Varying the time of extinction led to somewhat less intuitive results, mainly because of a rapidly evolving environmental context of deglacial climate change. An earlier extinction by some 3000 yr (15 ky BP) yielded a global temperature anomaly comparable to that computed with the MIS, however no cold pocket was present in the Weddell Sea. We hypothesize that slightly lower global temperatures during that period (and therefore a lower freshwater flux into the North Atlantic Ocean) prevented a weakening of the

Title Page
Abstract | Introduction
Conclusions | References
Tables | Figures
◀| |▶
◀ ▶
Back | Close
Full Screen / Esc
Printer-friendly Version
Interactive Discussion

thermohaline circulation, hence the small difference between either experiments after 500 yr of climate model simulation. As expected, a later extinction by 2000 yr (10 ky BP) resulted in further enhanced SAT anomalies compared to the MIS. The spatial distribution of temperature anomalies was slightly different at the northern high latitudes due to the disappearance of a moderately large fraction of the continental ice sheets between 12 ky BP and 10 ky BP (prescribed in the UVic ESCM), which opened up more territory for the northward expansion of vegetation.

6.2 Biogeophysical vs. biogeochemical effects: results from a "free CO_2" experiment

Throughout all of the above experiments, carbon dioxide levels were prescribed in the atmosphere in order to obtain a climatic response attributable to biogeophysical effects only. Here, we allowed CO_2 levels to fluctuate based on land cover changes in an attempt to quantify the combined biogeophysical and biogeochemical effects of the extinction-induced changes in vegetation cover. For the sake of consistency (and an easier comparison), we have chosen to repeat the experimental setup for the MIS.

Results from this simulation, displayed in Fig. 6, are surprising. We would have expected the temperature response from biogeophysical effects to be at least partly offset by carbon cycle effects due to the increased carbon sequestration of trees and shrubs. Instead, both effects appear to enhance each other, resulting in a combined warming that nearly doubles that from biogeophysical effects alone (Fig. 6a). The CO_2 anomaly curve (Fig. 6b) follows a pattern slightly different to that of temperature and surface albedo for the MIS experiment: atmospheric CO_2 levels increased by about 15 ppm in the first 150 yr following the extinction, after which the trend reversed (attributable to an increase in carbon sequestration). However, the overall anomaly for the 500 climate model years of the simulation was still overwhelmingly positive.

An analysis of carbon fluxes between the land and atmosphere revealed that the initial increase in CO_2 was closely related to the vegetation change. While this could seem obvious at first glance due to the nature of the experiment, it appears that the

UVic model and TRIFFID in particular, defines various limits for soil carbon content depending on the dominant PFT. Since this limit is lower for shrubs than for C3 grasses, the replacement of grass by shrubs in several grid cells north of 30° N would have caused a substantial release of soil carbon to the atmosphere. The change in soil carbon content (Fig. 6c) was found to overcompensate for the increase in vegetation carbon (Fig. 6d), and therefore the surplus likely accounted for most of the terrestrial carbon loss to the atmosphere.

It is difficult at this point to determine whether the carbon cycle response to the vegetation change in this model reflects a potential real-world effect. It is consistent, however, with previous studies which have shown the potential for significant soil carbon losses associated with vegetation transitions (e.g. Cox et al., 2001). In addition, there is evidence that real-world natural grasslands sequester large amounts of soil carbon (e.g. De Deyn et al., 2008), and so it is plausible that the replacement of grass-dominated ecosystems with shrub land may have led to an initial increase in atmospheric CO_2 as shown in our results.

7 Conclusions

This paper investigates biogeophysical and biogeochemical effects of faunal and floral changes on climate in the context of the Late Quaternary Extinctions and provides a quantitative assessment of those feedbacks in terms of surface albedo and temperature. To this end, we established an experimental strategy using a land-cover perturbation to represent the stress on high-latitude vegetation due to megafaunal herbivory. This setup was then used to explore several hypothetical cases of the mammoth extinction, including a catastrophic Maximum Impact Scenario (MIS) and a collection of more realistic variations of the former.

For the MIS we found the change in temperature following the mammoth extinction to be dominated by radiative effects, with an estimated surface warming of 0.175 °C globally and 0.420 °C over the mammoth area. Most of the warming could be linked to changes in vegetation, either as a direct consequence of reforestation or as a result of global warming through the expansion of hospitable terrain for trees and shrubs. As outlined in previous studies (Thomas and Rowntree, 1992; Bonan et al., 1992; Douville and Royer, 1996) the warming was found to be most pronounced in winter and spring, during which the albedo difference is greatest between the snow-covered ground and the dark forest canopy. Although positive anomalies dominated worldwide, cooling was observed in the Weddell Sea, a likely indicator of reduced deep water formation in the Southern Ocean.

In general, the range of sensitivity studies produced fairly intuitive results. The amplitude of the temperature response displayed a monotonic, albeit slightly nonlinear, dependency on both the size of mammoth habitat as well as the tree clearance ratio. Displacing the timing of extinction by a few thousand years did not appear to yield a significant difference with the MIS. However, a simulation of free carbon exchanges with the atmosphere yielded unexpected results, as the reforestation was found to coincide with a significant input of CO_2 in the atmosphere, most of it originating from the land surface reservoir.

Due to a strong height-based plant dominance hierarchy in TRIFFID, shrub types had mostly recovered their standard distribution within 100 yr of the mammoth extinction, perhaps too quickly for a natural reforestation. As expected due to the nature of our experiment, most of the albedo and temperature response was found to happen during this initial 100-yr regrowth. The remnants of LGM ice sheets were found to significantly influence the model output, especially in North America where potential reforestation was hampered by the massive Laurentide ice sheet. Our results also suggest that late Pleistocene boundary conditions led to a much later spring in the northern high latitudes, with spring snowmelt delayed by as much as several months compared to the present day.

In order to elaborate these results, it would be of interest to carry out simulations of the megafaunal extinctions with a more detailed representation of atmospheric dynamics. Such studies could also integrate realistic tree-mammoth scenarios with a predator-prey model, something that was disregarded in the present study for the sake of simplicity. Finally, we recommend a more thorough investigation of land surface processes and large-scale vegetation changes, as most of the more counterintuitive results obtained here originated from an abrupt change in the dominant PFT.

Acknowledgements. This paper is based on a thesis prepared by Marc-Olivier Brault during spring 2012 for the fulfillment of his MSc degree at McGill University. We are indebted to Jaime Palter for her helpful comments on the thesis manuscript, and to Michael Havas for technical assistance. Special thanks to Eric Galbraith for helpful tips in finding the cause of the cold anomaly in the Weddell Sea. The support of a Natural Sciences and Engineering Research Council (NSERC) Discovery Grant awarded to LAM, and a research scholarship awarded to M.-O. B. by the Global Environmental and Climate Change Centre (GEC3) for this work is greatly appreciated.

References

Alroy, J.: A multispecies overkill simulation of the end-Pleistocene megafaunal mass extinction, Science, 292, 1893–1896, 2001.

Bala, G., Caldeira, K., Wickett, M., Phillips, T. J., Lobell, D. B., Delire, C., and Mirin, A.: Combined climate and carbon-cycle effects of large-scale deforestation, Proc. Natl. Acad. Sci. USA, 104, 6550–6555, 2007.

Barnosky, A. D., Koch, P. L., Feranec, R. S., Wing, S. L., and Shabel, A. B.: Assessing the causes of late Pleistocene extinctions on the continents, Science, 306, 70–75, 2004.

Bitz, C. M., Holland, M. M., Weaver, A. J., and Eby, M.: Simulating the ice-thickness distribution in a coupled climate model, J. Geophys. Res., 106, 2441–2463, 2001.

Bonan, G. B., Pollard, D., and Thompson, S. L.: Effects of boreal forest vegetation on global climate, Nature, 359, 716–718, 1992.

Bonan, G. B., Chapin III, F. S., and Thompson, S. L.: Boreal forests and tundra ecosystems as components of the climate system, Clim. Change, 29, 145–167, 1995.

Brovkin, V., Levis, S., Loutre, M.-F., Crucifix, M., Claussen, M., Ganopolski, A., Kubatzki, C., and Petoukhov, V.: Stability analysis of the climate-vegetation system in the northern high latitudes, Clim. Change, 57, 119–138, 2003.

Brovkin, V., Raddatz, T., Reick, C. H., Claussen, M., and Gayler, V.: Global biogeophysical interactions between forest and climate, Geophys. Res. Lett., 36, L07405, doi:10.1029/2009GL037543, 2009.

Chalita, S. and Le Treut, H.: The albedo of temperate and boreal forest and the Northern Hemisphere climate: a sensitivity experiment using the LMD GCM, Clim. Dynam., 10, 231–240, 1994.

Cox, P.: Description of the“TRIFFI” Dynamic Global Vegetation Model, Met Office, Hadley Centre technical note 24, 2001.

Cox, P. M., Betts, R. A., Bunton, C. B., Essery, R. L., Rowntree, P. R., and Smith, J.: The impact of new land surface physics on the GCM simulation of climate and climate sensitivity, Clim. Dynam., 15, 183–203, 1999.

Cox, P. M., Betts, R. A., Jones, C. D., Spall, S. A., and Totterdell, I. J.: Modelling vegetation and the carbon cycle as interactive elements of the climate system, Met Office, Hadley Centre technical note 23, 2001.

Crucifix, M., Betts, R. A., and Hewitt, C. D.: Pre-industrial-potential and Last Glacial Maximum global vegetation simulated with a coupled climate-biosphere model: Diagnosis of bioclimatic relationships, Glob. Planet. Change, 45, 295–312, 2005.

Davin, E. L. and de Noblet-Ducoudré, N.: Climatic impact of global-scale deforestation: radiative versus nonradiative processes, J. Climate, 23, 97–112, 2010.

De Deyn, G. B., Cornelissen, J. H., and Bardgett, R. D.: Plant functional traits and soil carbon sequestration in contrasting biomes, Ecol. Lett., 11, 516–531, 2008.

Doughty, C. E., Wolf, A., and Field, C. B.: Biophysical feedbacks between the Pleistocene megafauna extinction and climate: The first human-induced global warming?, Geophys. Res. Lett., 37, L15703, doi:10.1029/2010GL043985, 2010.

Douville, H. and Royer, J.-F.: Influence of the temperate and boreal forests on the Northern Hemisphere climate in the Météo-France climate model, Clim. Dynam., 13, 57–74, 1997.

Eby, M., Zickfeld, K., Montenegro, A., Archer, D., Meissner, K. J., and Weaver, A. J.: Lifetime of anthropogenic climate change: millenial time scales of potential CO_2 and surface temperature perturbations, J. Climate, 22, 2501–2511, 2009.

Fanning, A. F. and Weaver, A. J.: An atmospheric energy-moisture balance model: climatology, interpentadal climate change, and coupling to an ocean general circulation model, J. Geophys. Res., 128, 15111–15128, 1996.

Foley, J. A., Prentice, I. C., Ramankutty, N., Levis, S., Pollard, D., Sitch, S., and Haxeltine, A.: An integrated biosphere model of land surface processes, terrestrial carbon balance, and vegetation dynamics, Global Biogeochem. Cy., 10, 603–628, 1996.

Foley, J. A., Costa, M. H., Delire, C., Ramankutty, N., and Snyder, P.: Green surprise? How terrestrial ecosystems could affect earth's climate, Front. Ecol. Environ., 1, 38–44, 2003.

Fraedrich, K., Jansen, H., Kirk, E., and Lunkeit, F.: The Planet Simulator: Green planet and desert world, Meteorol. Z., 14, 305–314, 2005.

Gibbard, S., Caldeira, K., Bala, G., Phillips, T. J., and Wickett, M.: Climate effects of global land cover change, Geophys. Res. Lett., 32, L23705, doi:10.1029/2005GL024550, 2005.

Grayson, D. K. and Meltzer, D. J.: A requiem for North American overkill, J. Archaeol. Sci., 30, 585–593, 2003.

Guthrie, R. D.: New carbon dates like climatic change with human colonization and Pleistocene extinctions, Nature, 441, 207–209, 2006.

Heck, P., Lüthi, D., Wernli, H., and Schär, C.: Climate impacts of European-scale anthropogenic vegetation changes: A sensitivity study using a regional climate model, J. Geophys. Res., 106, 7817–7835, 2001.

Kabat, P., Claussen, M., Dirmeyer, P. A., Gash, J. H. C., de Guenni, L. B., Meybeck, M., Vörösmarty, C. J., Hutjes, R. W. A. and Lütkemeier, S.: Vegetation, water, humans and the climate: A new perspective on an interactive system, in: Global Change, The IGBP Series, edited by: Springer, Berlin, p. 566, 2004.

Koch, P. L. and Barnosky, A. D.: Late Quaternary Extinctions: state of the debate, Annu. Rev. Ecol. Evol. Syst., 37, 215–250, 2006.

Martin, P. S.: Twilight of the Mammoths: Ice Age Extinctions and the Rewilding of America, Berkely, CA, Univ. of California Press, 2005.

Matthews, H. D., Weaver, A. J., Meissner, K. J., Gillett, N. P., and Eby, M.: Natural and anthropogenic climate change: incorporating historical land cover change, vegetation dynamics and the global carbon cycle, Clim. Dynam., 22, 461–479, 2004.

Matthews, H. D., Weaver, A. J., and Meissner, K. J.: Terrestrial carbon cycle dynamics under recent and future climate change, J. Climate, 18, 1609–1628, 2005.

Meissner, K. J., Weaver, A. J., Matthews, H. D., and Cox, P. M.: The role of land surface dynamics in glacial inception: a study with the UVic Earth System Model, Clim. Dynam., 21, 515–537, 2003.

Notaro, M. and Liu, Z.: Statistical and dynamical assessment of vegetation feedbacks on climate over the boreal forest, Clim. Dynam., 31, 691–712, 2008.

Owen-Smith, N.: Pleistocene extinctions: the pivotal role of megaherbivores, Paleobiology, 13, 351–362, 1987.

Peltier, W. R.: Ice age paleotopography, Science, 265, 195–201, 1994.

Petit, J. R., Jouzel, J., Raynaud, D., Barkov, N. I., Barnola, J.-M., Basile, I., Bender, M., Chappellaz, J., Davis, M., Delaygue, G., Delmotte, M., Kotlyakov, V. M., Legrand, M., Lipenkov, V. Y., Lorius, C., Pépin, L., Ritz, C., Saltzman, E., and Stievenard, M.: Climate and atmospheric history of the past 420 000 years from the Vostok ice core, Antarctica, Nature, 399, 429–436, 1999.

Prentice, I. C., Sykes, M. T., and Cramer, W.: The possible dynamic response of northern forests to global warming, Glob. Ecol. Biogeogr. Lett., 1, 129–135, 1991.

Prescott, G. W., Williams, D. R., Balmford, A., Green, R. E., and Manica, A.: Quantitative global analysis of the role of climate and people in explaining late Quaternary megafaunal extinctions, Proc. Natl. Acad. Sci. USA, 109, 4527–4531, 2012.

Schmittner, A., Oschlies, A., Matthews, H. D., and Galbraith, E. D.: Future changes in climate, ocean circulation, ecosystems, and biogeochemical cycling simulated for a business-as-usual CO_2 emission scenario until year 4000 AD, Global Biogeochem. Cy., 22, GB1013, doi:10.1029/2007GB002953, 2008.

Simmons, C. T., Mysak, L. A., and Matthews, H. D.: The role of Antarctic ice shelves in Holocene CO_2 concentrations: a study using the University of Victoria Earth System Climate Model, Poster presented at the annual meeting of the European Geosciences Union, Vienna, Austria, 2012.

Snyder, P. K., Delire, C., and Foley, J. A.: Evaluating the influence of different vegetation biomes on the global climate, Clim. Dynam., 23, 279–302, 2004.

Thomas, G. and Rowntree, P. R.: The boreal forests and climate, Q. J. R. Meteorol. Soc., 118, 469–497, 1992.

Weaver, A. J., Eby, M., Wiebe, E. C., Bitz, C. M., Duffy, P. B., Ewen, T. L., Fanning, A. F., Holland, M. M., MacFadyen, A., Matthews, H. D., Meissner, K. J., Saenko, O., Schmittner, A., Wang, H., and Yoshimori, M.: The UVic Earth System Climate Model: model description, climatology, and applications to past, present and future climates, Atmos. Ocean, 39, 361–428, 2001.

Wroe, S., Field, J., Fullagar, R., and Jermin, L. S.: Megafaunal extinction in the late Quaternary and the global overkill hypothesis, in: Alcheringa, An Australasian Journal of Palaeontology, 291–331, London, T. & F., 2004.

Table 1. List of sensitivity tests, described according to the three aspects selected for this study: year of extinction, tree clearance fraction, and southern extent of mammoth habitat. Parameterizations for the MIS are also shown for the sake of comparison.

Description	Year of extinction	Fraction of trees cleared	Southern extent of habitat
Maximum Impact Scenario	−12 000	1.00	30° N
30 % Reduced Herbivory	−12 000	0.70	30° N
60 % Reduced Herbivory	−12 000	0.40	30° N
45° N Habitat Limit	−12 000	1.00	45° N
60° N Habitat Limit	−12 000	1.00	60° N
Later Extinction	−10 000	1.00	30° N
Earlier Extinction	−15 000	1.00	30° N

Title Page
Abstract | Introduction
Conclusions | References
Tables | Figures
|◀ | ▶|
◀ | ▶
Back | Close
Full Screen / Esc
Printer-friendly Version
Interactive Discussion

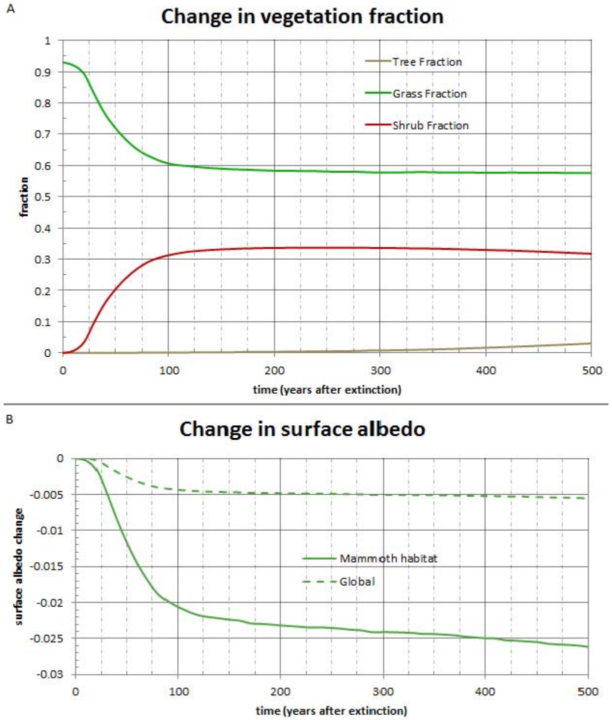

Fig. 1. Timeseries depicting the change in **(A)** vegetation fraction for every main vegetation type and **(B)** surface albedo both globally and over both the region of mammoth habitat (all land north of 30° N) as simulated by the UVic ESCM for MIS boundary conditions. This figure and every subsequent one represent the difference between a simulation where mammoths go extinct, and a simulation where their extinction does not occur.

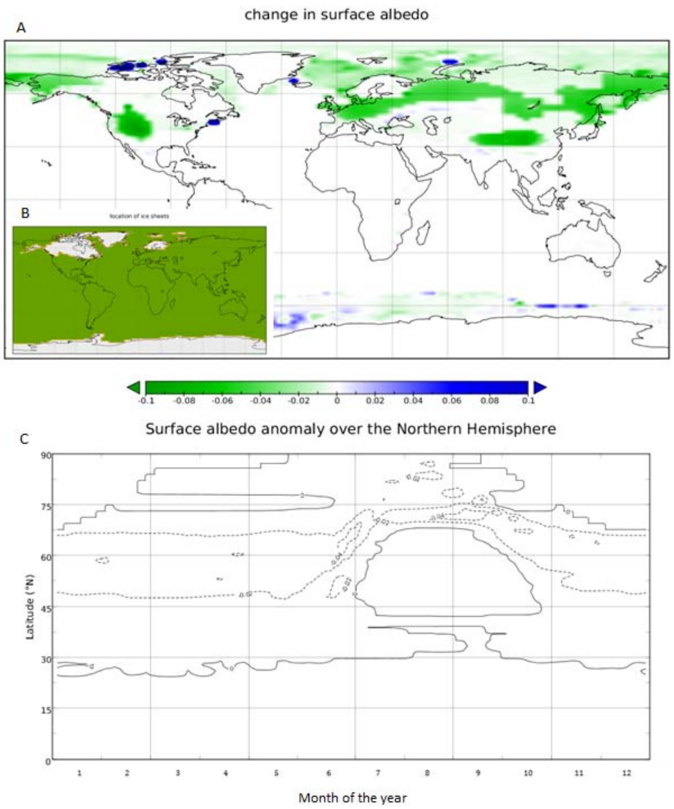

Fig. 2. Spatial distribution of **(A)** albedo changes after 500 yr of climate model simulations and **(B)** prescribed ice sheets at the end of the simulation. **(C)** Annual cycle of land surface albedo anomaly (EXT-CTL) in the Northern Hemisphere during the last year of climate model simulations. Solid line represent positive contours, while dotted lines represent negative values. On the abscissa, months are displayed from January to December according to their numerical order.

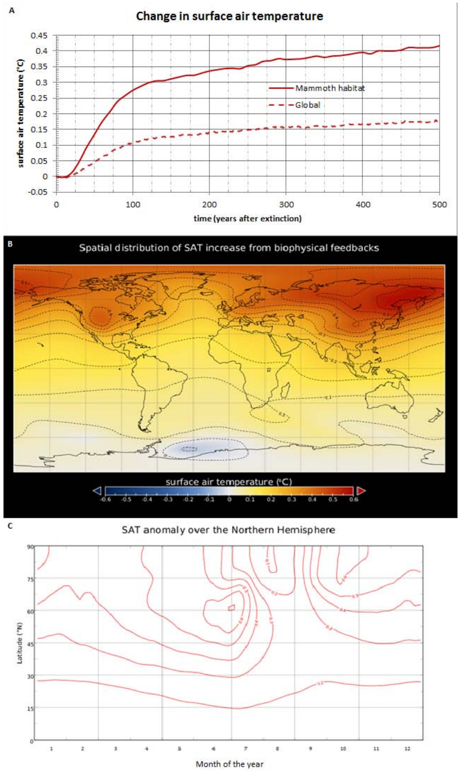

Fig. 3. Temperature anomalies between the EXT and CTL simulations with MIS boundary conditions. The data is presented here is the form of **(A)** a globally-averaged timeseries, **(B)** a annually-averaged spatial distribution at the end of the simulation, and **(C)** a zonally-averaged, annual cycle of temperature anomalies over the Northern Hemisphere. In frame **(C)**, the contour interval of the isotherms is 0.1 °C, and months on the abscissa are displayed from January to December in their numerical order.

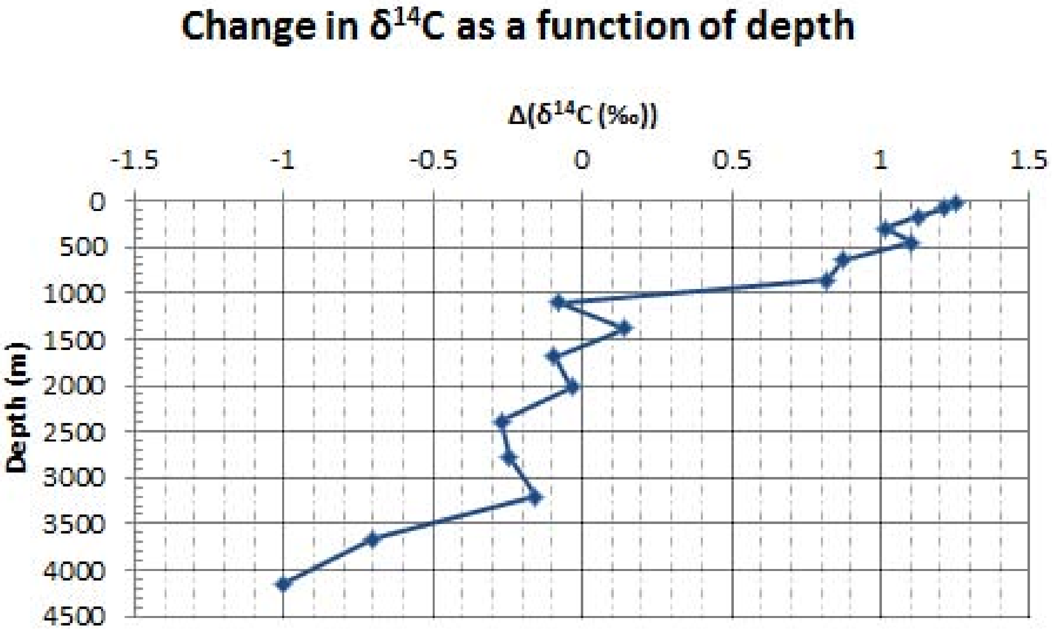

Fig. 4. Variations in δ^{14}C anomaly as a function of depth. This particular snapshot is taken in the Weddell Sea, in the middle of the cold anomaly visible in Fig. 3b, and averaged for the entire last year of the simulation.

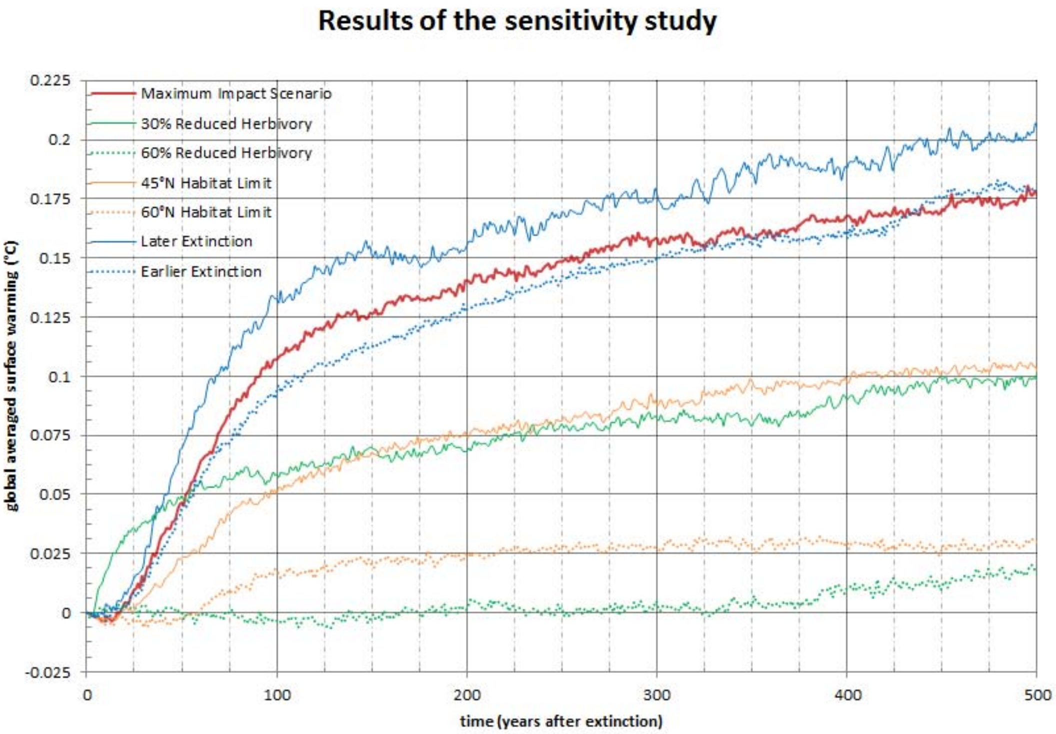

Fig. 5. Results of the sensitivity tests, presented here as a timeseries of temperature anomalies. The maximum impact scenario is shown in red for the sake of comparison.

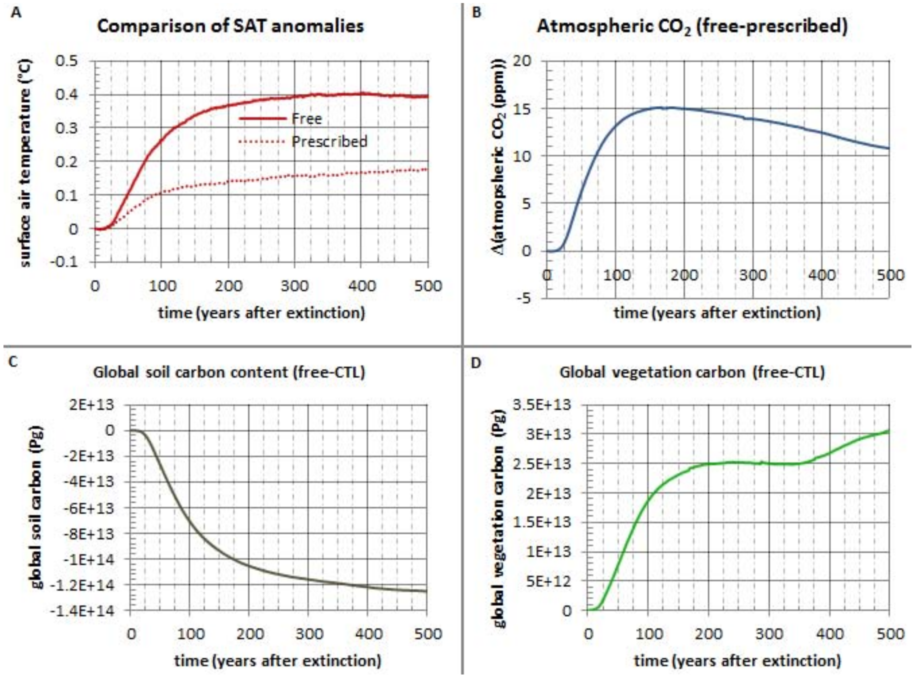

Fig. 6. A selection of results from the "free CO_2" experiment. Displayed are **(A)** a comparison of the temperature anomaly between the free and prescribed CO_2 experiments; **(B)** difference in atmospheric CO_2 between the two simulations; **(C)** change in total soil carbon and **(D)** total vegetation carbon resulting from the vegetation change.